Int. J. Solids Structures Vol. 26, No. 5/6, pp. 571–580, 1990
Printed in Great Britain.

0020–7683/90 $3.00+ .00

DIVERGENCE INSTABILITY OF REINFORCED COMPOSITE CIRCULAR CYLINDRICAL SHELLS†

VICTOR BIRMAN
University of Missouri–Rolla, Engineering Education Center, 8001 Natural Bridge Road, St Louis, MO 63121, U.S.A.

(*Received* 2 *August* 1988; *in final form* 19 *July* 1989)

Abstract—Divergence instability of a simply supported orthotropic composite shell reinforced in both axial and circumferential directions is considered. The shell is subject to an axial static load and to the action of an external supersonic gas flow in the direction parallel to the shell axis. Two variants of the solution considered in the paper include discrete widely spaced stiffeners and closely spaced stiffeners; the latter case can be treated using a smeared stiffeners technique.

INTRODUCTION

The problems of panel flutter and quasistatic aeroelastic instability (divergence) of composite structures have been intensively studied due to the increasing use of composites in aerospace applications. The outline of these studies including research concerning divergence instability was published in an excellent monograph of Librescu (1975). An example of the approach to the problems of divergence instability in design is the paper of Librescu and Simovich (1986).

Notably, the solutions of the problems of statics and dynamics of composite shells and plates, including aeroelastic problems, are usually limited to unreinforced structures. The number of works concerned with the behavior of reinforced composite shells and plates is small. In particular, Nguen-Fuk-Nin' and Marchenko (1970) considered the problem of flutter of an orthotropic cantilever plate with stiffener ribs in the case of a gas flow parallel to the ribs. The problem of axisymmetric divergence instability of orthotropic cylindrical shells reinforced by ring stiffeners was discussed by Birman (1988).

In this paper asymmetric divergence instability of orthotropic shells reinforced by both ring and axial stiffeners is considered. The solution is obtained using a two-term approximation for each component of the displacement field.

GOVERNING EQUATIONS

Consider a cylindrical shell reinforced internally in the axial and circumferential directions. The shell is symmetrically laminated of orthotropic laminae. The classical Donnell-type theory is used in the analysis. The shell is subject to an axial load with the stress resultant N_1 (positive in tension) and to the action of an external supersonic gas flow in the direction parallel to the shell axis. If the shell is thin, the effects of transverse shear can be neglected. Then the equations of equilibrium are

$$N_{x,x}+N_{xy,y}=0$$
$$N_{xy,x}+N_{y,y}=0$$
$$-M_{x,xx}+2M_{xy,xy}-M_{y,yy}+\frac{N_y}{R}-N_1 w_{,xx}=q \tag{1}$$

where N_x, N_y and N_{xy} are in-plane stress resultants, M_x, M_y and M_{xy} are the stress couples, q is the intensity of aerodynamic loading, and R is the middle surface radius. The stress

† This paper was presented at the ASME Winter Annual Meeting (Chicago, December 1988).

resultants and the stress couples are related to the displacements of the middle surface u, v, w by the constitutive relationships, Block (1968):

$$N_x = A_{11}u_{,x} + A_{12}(v_{,y} + w/R) + \sum_s \delta(y - y_s)E_sA_s(u_{,x} - z_sw_{,xx})$$

$$N_y = A_{12}u_{,x} + A_{22}(v_{,y} + w/R) + \sum_r \delta(x - x_r)E_rA_r(v_{,y} + w/R - z_rw_{,yy})$$

$$N_{xy} = A_{66}(u_{,y} + v_{,x})$$

$$M_x = -D_{11}w_{,xx} - D_{12}w_{,yy} + \sum_s \delta(y - y_s)[-E_sI_{0s}w_{,xx} + E_sA_sz_su_{,x}]$$

$$M_y = -D_{12}w_{,xx} - D_{22}w_{,yy} + \sum_r \delta(x - x_r)[-E_rI_{0r}w_{,yy} + E_rA_rz_r(v_{,y} + w/R)]$$

$$M_{xy} = 2D_{66}w_{,xy} + (1/2)\sum_r \delta(x - x_r)G_rJ_rw_{,xy} + (1/2)\sum_s \delta(y - y_s)G_sJ_sw_{,xy} \tag{2}$$

where δ is the Dirac delta function.

In (2) A_{ij} and D_{ij} are extensional and bending stiffnesses:

$$(A_{ij}, D_{ij}) = \int_h Q_{ij}(1, z^2)\,dz \tag{3}$$

where Q_{ij} are the corresponding transformed reduced stiffnesses, h is the thickness of the shell and z is the radial coordinate across the thickness of the shell.

The coordinates of the ring and axial stiffeners are denoted by x_r and y_s respectively. The moduli of elasticity of these stiffeners and their shear moduli are E_r, E_s, G_r and G_s. The moments of inertia of the stiffeners about the middle surface of the shell are I_{0r} (ring) and I_{0s} (axial stiffener). The torsional constants are denoted by J_r and J_s for ring and axial stiffeners respectively. z_r and z_s indicate the distance between the middle surface of the shell and the centroids of the corresponding stiffeners; the values of z_r and z_s are negative in case of internal stiffening.

The substitution of (2) into (1) yields the following set of equations of motion in displacements:

$$A_{11}u_{,xx} + A_{66}u_{,yy} + (A_{12} + A_{66})v_{,xy} + (A_{12}/R)w_{,x} + \sum_s \delta(y - y_s)E_sA_s(u_{,xx} - z_sw_{,xxx}) = 0$$

$$(A_{12} + A_{66})u_{,xy} + A_{22}v_{,yy} + A_{66}v_{,xx} + (A_{22}/R)w_{,y} + \sum_r \delta(x - x_r)E_rA_r(v_{,yy} + w_{,y}/R - z_rw_{,yyy}) = 0$$

$$D_{11}w_{,xxxx} + 2(D_{12} + 2D_{66})w_{,xxyy} + D_{22}w_{,yyyy} + (A_{12}/R)u_{,x}$$
$$+ (A_{22}/R)v_{,y} + (A_{22}/R^2)w + \sum_r \delta(x - x_r)[G_rJ_rw_{,xxyy}$$
$$+ E_rI_{0r}w_{,yyyy} + E_rA_r(v_{,y}/R + w/R^2 - 2z_rw_{,yy}/R - z_rv_{yyy})]$$
$$+ \sum_s \delta(y - y_s)(G_sJ_sw_{,xxyy} + E_sI_{0s}w_{,xxxx} - E_sA_sz_su_{,xxx}) - N_1w_{,xx} = q. \tag{4}$$

Notably, if the torsional stiffnesses of the reinforcement elements are neglected, these equations can be reduced to equations for ring-stiffened or axially stiffened shells used by Bogdanovich and Koshkina (1983, 1984) or to the equations for the shells reinforced in both directions, see Bogdanovich (1986).

The load induced by a gas flow is described by the piston theory:

$$q = \rho_a c^2 \bar{M} w_{,x} \tag{5}$$

where ρ_a is the density of air, c is the sound velocity and $\bar{M}$ is a speed parameter depending on the Mach number:

$$\bar{M} = M^2(M^2-1)^{-1/2}. \tag{6}$$

The shell is simply supported at the end cross sections. In-plane boundary conditions are

$$N_x = v = 0 \quad \text{at} \quad x = 0, \quad x = L. \tag{7}$$

These boundary conditions denoted S2 (Almroth, 1966), or SS3 (Hoff, 1965) are satisfied by the representation of the displacements field by two successive modes which is typical in aeroelastic applications, Librescu (1975), p. 73. This representation also satisfies the periodicity requirement in the circumferential direction:

$$\begin{aligned} u &= [U_m \cos m\pi x/L + U_{m+1} \cos (m+1)\pi x/L] \sin ny/R \\ v &= [V_m \sin m\pi x/L + V_{m+1} \sin (\mathrm{m}+1)\pi x/L] \cos ny/R \\ w &= [W_m \sin m\pi x/L + W_{m+1} \sin (m+1)\pi x/L] \sin ny/R \end{aligned} \tag{8}$$

where m and n are positive integers.

ANALYSIS OF SHELLS WITH DISCRETE STIFFENERS

Substitution of eqns (5) and (8) into eqns (4) followed by the application of Galerkin's procedure yields the following set of six equations:

$$\begin{aligned} &[k_{11}^{(i)} + s_{11}^{(i)}]\bar{U}_i + k_{12}^{(i)}\bar{V}_i = [k_{13}^{(i)} + s_{13}^{(i)}]\bar{W}_i \\ &k_{21}^{(i)}\bar{U}_i + k_{22}^{(i)}\bar{V}_i + \sum_{j=m}^{m+1} s_{22}^{(ij)}\bar{V}_j = k_{23}^{(i)}\bar{W}_i + \sum_{j=m}^{m+1} s_{23}^{(ij)}\bar{W}_j \\ &[k_{33}^{(i)} + s_{33}^{(i)} + \bar{N}_1(i\pi\bar{h})^2]\bar{W}_i + \sum_{j=m}^{m+1} s_{ss}^{(ij)}\bar{W} - [k_{31}^{(i)} + s_{31}^{(i)}]\bar{U}_i - k_{32}^{(i)}\bar{V}_i - \sum_{j=m}^{m+1} s_{32}^{(ij)}\bar{V}_j = F(\bar{W}_i) \end{aligned} \tag{9}$$

where $i = m, m+1$ while $(\bar{U}_i, \bar{V}_i, \bar{W}_i)$ denote the nondimensional amplitudes defined as

$$(\bar{U}_i, \bar{V}_i, \bar{W}_i) = (U_i, V_i, W_i)/h. \tag{10}$$

The function $F(\bar{W}_i)$ is defined as

$$F(\bar{W}_i) = \begin{cases} f_{33}\bar{M}\bar{W}_{m+1} & \text{if} \quad i = m \\ -f_{33}\bar{M}\bar{W}_m & \text{if} \quad i = m+1 \end{cases} \tag{11}$$

where

$$f_{33} = 4m(m+1)\bar{\rho}_a\bar{h}/(2m+1) \tag{12}$$

and

$$\bar{\rho}_a = \rho_a c^2/E_T \quad \bar{h} = h/L \tag{13}$$

E_T being tangential Young's modulus in the direction perpendicular to the fibers. The nondimensional axial load resultant is

$$\bar{N}_1 = N_1/E_T h. \tag{14}$$

The coefficients $k_{\alpha\beta}^{(i)}$, $s_{\alpha\beta}^{(i)}$ and $s_{\alpha\beta}^{(ij)}$ in (9) are given in Appendix A. The nondimensional amplitudes of harmonics of the in-surface displacements can be expressed from the first two couples of eqns (9); i.e. from the first two equations for $i = m$ and $i = m+1$:

$$\begin{aligned}
\bar{U}_m &= R_1^{(m)} \bar{W}_m + R_2^{(m)} \bar{W}_{m+1} \\
\bar{V}_m &= R_3^{(m)} \bar{W}_m + R_4^{(m)} \bar{W}_{m+1} \\
\bar{U}_{m+1} &= R_1^{(m+1)} \bar{W}_m + R_2^{(m+1)} \bar{W}_{m+1} \\
\bar{V}_{m+1} &= R_3^{(m+1)} \bar{W}_m + R_4^{(m+1)} \bar{W}_{m+1}
\end{aligned} \tag{15}$$

where the coefficients $R_i^{(j)}$ are given in Appendix B. The substitution of (15) into the last equation (9) when $i = m$ and $i = m+1$ yields

$$\begin{aligned}
T_1 \bar{W}_m + T_2 \bar{W}_{m+1} &= 0 \\
T_3 \bar{W}_m + T_4 \bar{W}_{m+1} &= 0.
\end{aligned} \tag{16}$$

The coefficients T_i are shown in Appendix C.

The nonzero requirement for $\bar{W}_m$ and $\bar{W}_{m+1}$ yields the condition of the divergence instability:

$$T_1 T_4 - T_2 T_3 = 0. \tag{17}$$

The values of the parameter $\bar{M}$ and the Mach numbers corresponding to divergence instability can be determined from (17).

APPLICATION OF SMEARED STIFFENERS TECHNIQUE

The smeared stiffeners technique is effective if the stiffeners in each direction have identical cross sections and their spacing is small. Sometimes this technique is used for the stiffeners in one direction while the stiffeners in another direction are treated as discrete, see Block (1968). If the number of stiffeners is small or the spacing is large, smeared stiffeners technique does not yield accurate results, Bogdanovich and Koshkina (1983; 1984). To apply this technique the sums of the delta functions in (4) must be replaced as follows:

$$\begin{aligned}
\sum_r \delta(x - x_r) &\to 1/l_r \\
\sum_s \delta(y - y_s) &\to 1/l_s
\end{aligned} \tag{18}$$

l_r and l_s being the spacings of the ring and axial stiffeners respectively. Then the substitution of (5) and (8) into the modified eqns (4) yields the following set of equations:

$$\begin{aligned}
[k_{11}^{(i)} + \tilde{s}_{11}^{(i)}]\bar{U}_i + k_{12}^{(i)} \bar{V}_i &= [k_{13}^{(i)} + \tilde{s}_{13}^{(i)}]\bar{W}_i \\
k_{21}^{(i)} \bar{U}_i + [k_{22}^{(i)} + \tilde{s}_{22}^{(i)}]\bar{V}_i &= [k_{23}^{(i)} + \tilde{s}_{23}^{(i)}]\bar{W}_i \\
[k_{33}^{(i)} + \tilde{s}_{33}^{(i)} + \bar{N}_1 (i\pi\bar{h})^2]\bar{W}_i - [k_{31}^{(i)} + \tilde{s}_{31}^{(i)}]\bar{U}_i - [k_{32}^{(i)} + \tilde{s}_{32}^{(i)}]\bar{V}_i &= F(\bar{W}_i).
\end{aligned} \tag{19}$$

The coefficients $\tilde{s}_{\alpha\beta}^{(i)}$ are given in Appendix D. The first two equations of (19) yield

$$\bar{U}_i = K_1^{(i)} \bar{W}_i$$
$$\bar{V}_i = K_2^{(i)} \bar{W}_i \tag{20}$$

where

$$K_1^{(i)} = \{[k_{13}^{(i)} + \tilde{s}_{13}^{(i)}][k_{22}^{(i)} + \tilde{s}_{22}^{(i)}] - k_{12}^{(i)}[k_{23}^{(i)} + \tilde{s}_{23}^{(i)}]\}/K$$
$$K_2^{(i)} = \{[k_{11}^{(i)} + \tilde{s}_{11}^{(i)}][k_{23}^{(i)} + \tilde{s}_{23}^{(i)}] - k_{21}^{(i)}[k_{13}^{(i)} + \tilde{s}_{13}^{(i)}]\}/K$$
$$K = [k_{11}^{(i)} + \tilde{s}_{11}^{(i)}][k_{22}^{(i)} + \tilde{s}_{22}^{(i)}] - k_{12}^{(i)} k_{21}^{(i)}. \tag{21}$$

The substitution of $\bar{U}_i$ and $\bar{V}_i$ into the last equation (19) when $i = m$ and $i = m+1$ yields:

$$P^{(m)} \bar{W}_m - f_{33} \bar{M} \bar{W}_{m+1} = 0$$
$$f_{33} \bar{M} \bar{W}_m + P^{(m+1)} \bar{W}_{m+1} = 0 \tag{22}$$

where

$$P^{(i)} = k_{33}^{(i)} + \tilde{s}_{33}^{(i)} + \bar{N}_1 (i\pi\bar{h})^2 - [k_{31}^{(i)} + \tilde{s}_{31}^{(i)}] K_1^{(i)} - [k_{32}^{(i)} + \tilde{s}_{32}^{(i)}] K_2^{(i)}. \tag{23}$$

The value $\bar{M}$ corresponding to divergence is

$$\bar{M} = [-P^{(m)} P^{(m+1)}]^{1/2} / f_{33}. \tag{24}$$

The necessary condition of the existence of divergence instability is obtained from (24):

$$\bar{N}_{1cr}^{(mn)} < \bar{N}_1 < \bar{N}_{1cr}^{((m+1)n)}$$

or

$$\bar{N}_{1cr}^{((m+1)n)} < \bar{N}_1 < \bar{N}_{1cr}^{(mn)} \tag{25}$$

depending on the relation between static buckling loads $\bar{N}_{1cr}^{(mn)}$ and $\bar{N}_{1cr}^{(m+1)}$. The static buckling load of the shell associated with the mode shape with i half-waves in the axial direction and n half-waves in the circumferential direction is obtained from (23):

$$\bar{N}_{1cr}^{(in)} = -\{k_{33}^{(i)} + \tilde{s}_{33}^{(i)} - [k_{31}^{(i)} + \tilde{s}_{31}^{(i)}] K_1^{(i)} - [k_{32}^{(i)} + \tilde{s}_{32}^{(i)}] K_2^{(i)}\} / (i\pi\bar{h})^2. \tag{26}$$

Note that (25) represents only the necessary condition of divergence instability. Such instability is possible only if the Mach number corresponding to $\bar{M}$ determined from (24) is real. This requirement is satisfied if $\bar{M} \geqslant 2$.

NUMERICAL EXAMPLES

The geometry of shells considered in examples was $L/R = 4$, $h/L = 0.005$. The stiffeners in the axial and circumferential directions had the following characteristics:

$$A_r/R^2 = A_s/R^2 = 0.002, \quad I_{0r}/(L^2R^2) = I_{0s}/(L^2R^2) = 55.42 \times 10^{-8},$$
$$J_r/(L^2R^2) = J_s/(L^2R^2) = 1.517 \times 10^{-8}, \quad \bar{z}_r = \bar{z}_s = -3.$$

The dimensionless spacing of the stiffeners was $l_r/L = l_s/L = 0.05$. Two materials were considered: E-glass/epoxy ($E_L = 7.8 \times 10^6$ psi, $E_T = 2.6 \times 10^6$ psi, $\nu_{LT} = 0.25$, $G_{LT} = 1.3 \times 10^6$ psi) and high-modulus graphite/epoxy ($E_L = 30 \times 10^6$ psi, $E_T = 0.75 \times 10^6$ psi, $\nu_{LT} = 0.25$, $G_{LT} = 0.375 \times 10^6$ psi). The lamination angle was $\pm 15°$ for E-glass/epoxy and $\pm 30°$ for high-modulus graphite/epoxy. The number of layers was supposed to be large so that

the shells could be treated as orthotropic. The results were obtained using smeared stiffeners technique. The control checks with the solution obtained for discrete stiffeners illustrated that smeared stiffeners technique is acceptable for the shells with the geometry indicated above.

The previous analysis showed the importance of determination of static buckling loads. They represent the boundaries of the intervals of external compressive loads where divergence instability is possible [see (25)]. The values of these loads are shown in Tables 1 and 2 for the shells reinforced in both directions. Two values of the buckling loads are given for each combination (m, n). The upper values correspond to the negligible torsional stiffness of reinforcements. The lower values were calculated taking torsional stiffness into account. The comparison of these values illustrates that the contribution of the torsional stiffness is negligible. The values of buckling loads for high-modulus graphite epoxy shells with the stiffeners in axial or circumferential directions only and for unreinforced shells are shown in Tables 3–5, respectively. The comparison of the smallest nondimensional buckling loads for graphite/epoxy shells follows:

Load	Mode	Reinforcements
−0.985	$m = n = 3$	in both directions
−0.101	$m = 1, n = 4$	axial stiffeners
−0.151	$m = 12, n = 3$	ring stiffeners
−0.066	$m = 8, n = 2$	shell unreinforced

This comparison illustrates the high effectiveness of stiffeners.

The values of the parameter $\bar{M}$ corresponding to divergence instability of a graphite/epoxy shell reinforced in both directions are shown in Fig. 1. As it is seen from this figure the values of $\bar{M}$ can be very high. For high Mach numbers, $\bar{M}$ could be approximated by M. The value $\ln \bar{M} = 0.693$ corresponds to $\bar{M} = 2$. Therefore the parts of the curves below this value must be disregarded. Compressive loads corresponding to limited Mach numbers which represent practical interest are within very narrow intervals located close to the buckling values. However this conclusion is correct only if the difference between

Table 1. Buckling loads of E-glass/epoxy shells reinforced in axial and circumferential directions, $|\bar{N}_{1cr}^{(mn)}|$; $(G_rJ_r = G_sJ_s = 0)/(G_rJ_r, G_sJ_s \neq 0)$.

	m									
n	1	2	3	4	5	6	7	8	9	10
2	0.152	0.108	0.107	0.116	0.133	0.158	0.191	0.231	0.278	0.332
	0.153	0.108	0.107	0.116	0.134	0.159	0.191	0.231	0.278	0.332
3	0.483	0.147	0.098	0.097	0.113	0.139	0.174	0.216	0.265	0.321
	0.484	0.148	0.099	0.097	0.113	0.140	0.175	0.217	0.266	0.322
4	1.475	0.387	0.199	0.150	0.144	0.159	0.187	0.225	0.272	0.325
	1.476	0.388	0.200	0.151	0.145	0.160	0.188	0.226	0.273	0.326

Table 2. Buckling loads of high-modulus graphite/epoxy shells reinforced in axial and circumferential directions, $|\bar{N}_{1cr}^{(mn)}|$; $(G_rJ_r = G_sJ_s = 0)/(G_rJ_r, G_sJ_s \neq 0)$.

	m									
n	1	2	3	4	5	6	7	8	9	10
2	1.500	1.161	1.182	1.307	1.528	1.842	2.241	2.723	3.282	3.918
	1.501	1.162	1.182	1.307	1.529	1.842	2.242	2.723	3.283	3.918
3	3.921	1.311	0.984	1.052	1.282	1.619	2.041	2.543	3.118	3.766
	3.922	1.313	0.985	1.053	1.283	1.619	2.042	2.543	3.119	3.767
4	11.445	3.109	1.800	1.541	1.618	1.862	2.222	2.677	3.216	3.836
	11.447	3.110	1.801	1.542	1.619	1.863	2.223	2.678	3.217	3.837

Table 3. Buckling loads of high-modulus graphite/epoxy shells reinforced in axial direction, $|\bar{N}_{1cr}^{(in)}|$.

	m									
n	1	2	3	4	5	6	7	8	9	10
2	0.722	0.995	0.934	1.064	1.319	1.669	2.099	2.605	3.184	3.835
3	0.140	0.443	0.670	0.894	1.186	1.554	1.995	2.507	3.091	3.744
4	0.101	0.188	0.409	0.687	1.014	1.401	1.854	2.374	2.962	3.619
5	0.176	0.159	0.283	0.517	0.838	1.230	1.688	2.213	2.805	3.465

Table 4. Buckling loads of high-modulus graphite epoxy shells reinforced in circumferential direction, $|\bar{N}_{1cr}^{(in)}|$.

	m								
n	8	9	10	11	12	13	14	15	16
2	0.311	0.270	0.241	0.221	0.209	0.202	0.200	0.201	0.206
3	0.184	0.166	0.156	0.152	0.151	0.153	0.159	0.166	0.176
4	0.201	0.177	0.164	0.157	0.156	0.159	0.164	0.172	0.181
5	0.398	0.342	0.304	0.280	0.264	0.255	0.251	0.251	0.254

Table 5. Buckling loads of unreinforced high-modulus graphite/epoxy shells, $|\bar{N}_{1cr}^{(in)}|$.

	m									
n	5	6	7	8	9	10	11	12	13	14
2	0.100	0.078	0.068	0.066	0.068	0.072	0.079	0.087	0.097	0.109
3	0.121	0.092	0.080	0.076	0.077	0.081	0.087	0.095	0.105	0.116
4	0.151	0.113	0.096	0.090	0.090	0.093	0.099	0.107	0.117	0.128
5	0.178	0.139	0.118	0.109	0.107	0.109	0.114	0.122	0.131	0.142

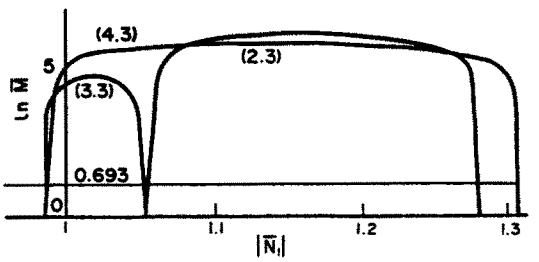

Fig. 1. Relationship between parameters $|\bar{N}_1|$ and $\bar{M}$ corresponding to divergence instability (high-modulus graphite/epoxy shell reinforced in axial and circumferential directions). The numbers in the curved brackets denote (m, n).

$\bar{N}_{1cr}^{(mn)}$ and $\bar{N}_{1cr}^{((m+1)n)}$ is significant. As it follows from Fig. 2 obtained for an E-glass/epoxy shell if the difference between the buckling loads is 0.56% ($m = n = 2$) the values of $\bar{M}$ remain small within the whole interval $(\bar{N}_{1cr}^{(2,2)}, \bar{N}_{1cr}^{(3,2)})$. If this difference increases to 1.62% ($m = n = 3$) the values of $\bar{M}$ increase as well but still remain limited.

The interior domains of the loops in Figs 1 and 2 correspond to the divergence instability. The maximum Mach numbers obtained from Figs 1 and 2 represent critical divergence velocities, see Librescu (1975, p. 87). If the gas velocity exceeds the critical divergence value, equilibrium with the corresponding mode shape becomes impossible.

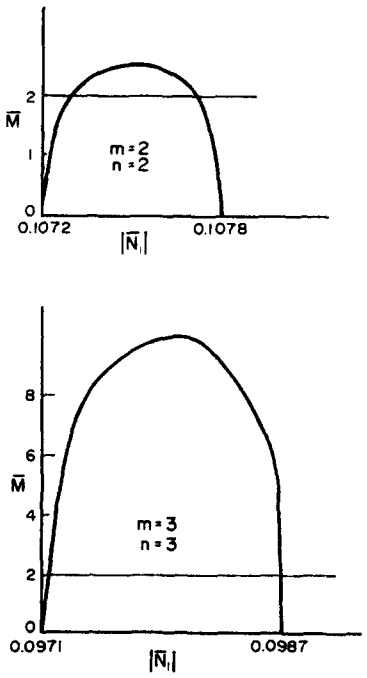

Fig. 2. Relationship between parameters $|\bar{N}_1|$ and $\bar{M}$ corresponding to divergence instability (E-glass/epoxy shell reinforced in axial and circumferential directions).

As shown in Figs 1 and 2 critical divergence velocities remain limited only if the buckling loads $\bar{N}_{1cr}^{(in)}$ corresponding to two subsequent modes ($i = m, m+1$) are very close. If this condition is not satisfied, the critical velocities are too high to represent practical interest.

Note that the mode shape of divergence, i.e. the values of m and n corresponding to the minimum divergence speed can be evaluated either by trials or minimizing the Mach number parameter $\bar{M}$ with respect to these variables. Due to complicated analytical relationships $\bar{M}(m, n)$ which are defined by (17) or (24) minimization appears to be unpractical. Instead the mode shape of divergence should be determined by trials. For example, in the case shown in Fig. 1 the mode shape of divergence at $\bar{N}_1 = -1.2$ has three half-waves in the circumferential direction and the combination of two and three half-waves in the axial direction.

It is important to understand the effect of the sequence of application of loads. If buckling loads are applied before the gas flow, the shell buckles and the present solution is not applicable. However, if the axial load is applied to the shell which is already experiencing the effect of flow (this can happen due to aerodynamic heating), the solution developed in the paper is valid.

CONCLUSIONS AND DISCUSSION

The problem of divergence instability of orthotropic cylindrical shells reinforced in the axial and circumferential directions is considered. It is shown that divergence instability of a shell with closely spaced stiffeners can occur only if it is subject to compressive loads exceeding the static buckling value. This means that the supersonic gas flow can have a stabilizing influence on compressed cylindrical shells. Notably, a similar conclusion was obtained in the previous work of the author, Birman (1988), dealing with axisymmetric divergence. In asymmetric and axisymmetric divergence problems these static buckling loads correspond to asymmetric and axisymmetric buckling mode shapes respectively. Since asymmetric buckling is usually reached at a smaller load than its axisymmetric counterpart in shells used in many practical applications, asymmetric divergence is more likely to occur in such shells. Within the intervals of compressive loads satisfying the necessary conditions

of divergence instability the Mach numbers corresponding to this instability can be very high. The effect of torsional stiffness of the stiffeners is shown to be negligible.

Acknowledgement—The author is grateful to Mr. Zouhair Said for his help in calculations.

REFERENCES

Almroth, B. O. (1966). Influence of edge conditions on the stability of axially compressed cylindrical shells. *AIAA J.* **4**, 134.

Birman, V. (1988). Axisymmetric divergence of ring-stiffened composite cylindrical shells subject to axial compression. *J. Appl. Mech.* **55**, 984.

Block, D. L. (1968). Influence of discrete ring stiffeners and prebuckling deformations on the buckling of eccentrically stiffened orthotropic cylinders, NASA TN D-4283.

Bogdanovich, A. E. and Koshkina, T. B. (1983). Deformation and strength of orthotropic cylindrical shells reinforced by ring stiffeners and subject to dynamic compressive loads. *Mechanics of Composite Materials* **3**, 476. In Russian.

Bogdanovich, A. E. and Koshkina, T. B. (1984). Deformation and strength of orthotropic cylindrical shells reinforced by axial stiffeners and subject to dynamic compressive loads. *Mechanics of Composite Materials* **5**, 866. In Russian.

Bogdanovich, A. E. (1986). Nonlinear problems of the dynamic buckling of reinforced laminar cylindrical shells. *Soviet Applied Mechanics* **22**(8), 745.

Hoff, N. J. (1965). Buckling of axially compressed circular cylindrical shells at stresses smaller than the classical value. *J. Appl. Mech.* **32**, 542.

Librescu, L. (1975). *Elastostatics and Kinetics of Anisotropic and Heterogeneous Shell-Type Structures*. Noordhoff Int. Publishing, Leyden.

Librescu, L. and Simovich, J. (1986). A general formulation for the aeroelastic divergence of composite swept-forward wing structures. Paper ICAS-86-4.8.2 at the 15th Congress of the International Council of the Aeronautical Sciences, London.

Nguen-Fuk-Nin' and Marchenko, G. A. (1970). Flutter of an orthotropic cantilever plate with stiffener ribs. *Soviet Applied Mechanics* **6**, 562.

APPENDIX A

The coefficients in (9):

$$
\begin{aligned}
k_{11}^{(i)} &= (i\pi\bar{h})^2\bar{A}_{11}+(n\lambda\bar{h})^2\bar{A}_{66}\\
k_{12}^{(i)} &= k_{21}^{(i)} = in\pi\lambda\bar{h}^2(\bar{A}_{12}+\bar{A}_{66})\\
k_{13}^{(i)} &= k_{31}^{(i)} = i\pi\lambda\bar{h}^2\bar{A}_{12}\\
k_{22}^{(i)} &= (i\pi\bar{h})^2\bar{A}_{66}+(n\lambda\bar{h})^2\bar{A}_{22}\\
k_{23}^{(i)} &= k_{32}^{(i)} = n(\lambda\bar{h})^2\bar{A}_{22}\\
k_{33}^{(i)} &= (i\pi\bar{h})^4\bar{D}_{11}+2(i\pi n\lambda)^2\bar{h}^4(\bar{D}_{12}+2\bar{D}_{66})+(n\lambda\bar{h})^4\bar{D}_{22}+(\lambda\bar{h})^2\bar{A}_{22}
\end{aligned}
\tag{A1}
$$

$$
\begin{aligned}
s_{11}^{(i)} &= (i^2\pi\bar{h}/\lambda)\sum_s \bar{E}_s\bar{A}_s\sin^2 ny_s/R\\
s_{13}^{(i)} &= [(i\pi\bar{h})^3\bar{z}_s/(\pi\lambda\bar{h})]\sum_s \bar{E}_s\bar{A}_s\sin^2 ny_s/R\\
s_{31}^{(i)} &= [(i\pi)^3\bar{h}^2/\pi\lambda^2]\sum_s \bar{E}_s\bar{A}_s\bar{z}_s\sin^2 ny_s/R\\
s_{33}^{(i)} &= (1/\pi)\sum_s\{(i\pi n)^2\lambda\bar{h}\bar{G}_s\bar{J}_s+[(i\pi)^4\bar{h}/\lambda]\bar{E}_s\bar{I}_{0s}\}\sin^2 ny_s/R
\end{aligned}
\tag{A2}
$$

$$
\begin{aligned}
s_{22}^{(ij)} &= 2n^2\bar{h}\sum_r \bar{E}_r\bar{A}_r\sin i\pi x_r/L\sin j\pi x_r/L\\
s_{23}^{(ij)} &= 2n\bar{h}\sum_r \bar{E}_r\bar{A}_r(1+n^2\bar{z}_r\lambda\bar{h})\sin i\pi x_r/L\sin j\pi x_r/L\\
s_{32}^{(ij)} &= (2n\bar{h}/\pi)\sum_r \bar{E}_r\bar{A}_r(1+n^2\bar{z}_r\lambda\bar{h})\sin i\pi x_r/L\sin j\pi x_r/L\\
s_{33}^{(ij)} &= (2\bar{h}/\pi)\sum_r[(j\pi n)^2\bar{G}_r\bar{J}_r+n^4\lambda^2\bar{E}_r\bar{I}_{0r}+\bar{E}_r\bar{A}_r(1+2\bar{z}_rn^2\lambda\bar{h})]\sin i\pi x_r/L\sin j\pi x_r/L.
\end{aligned}
\tag{A3}
$$

In (A1)–(A3)

$$(\bar{A}_{ij},\bar{D}_{ij}) = (A_{ij}/E_Th, D_{ij}/E_Th^3) \tag{A4}$$

$$\bar{h} = h/L,\quad \lambda = L/R$$

$$(\bar{z}_r,\bar{z}_s) = (z_r,z_s)/h \tag{A5}$$

$$
\begin{aligned}
(\bar{E}_r, \bar{E}_s) &= (E_r, E_s)\ E_T \\
(\bar{A}_r, \bar{A}_s) &= (A_r, A_s)\ R^2 \\
(\bar{G}_r, \bar{G}_s) &= (G_r, G_s)\ E_T \\
(\bar{J}_r, \bar{J}_s) &= (J_r, J_s)\ (L^2R^2) \\
(\bar{I}_{0r}, \bar{I}_{0s}) &= (I_{0r}, I_{0s})\ (L^2R^2)
\end{aligned} \tag{A6}
$$

APPENDIX B

The coefficients $R_i^{(j)}$ are

$$R_i^{(j)} = D_i^{(j)}/D$$

where

$$D = \begin{vmatrix} c_1 & c_2 & 0 & 0 \\ 0 & 0 & c_4 & c_5 \\ c_7 & c_8 & 0 & c_9 \\ 0 & c_{11} & c_{12} & c_{14} \end{vmatrix}.$$

The determinants $D_i^{(j)}$ are obtained from D where one of the columns is replaced by the columns indicated here as follows:

Determinant	$D_1^{(m)}$	$D_2^{(m)}$	$D_1^{(m+1)}$	$D_2^{(m+1)}$	$D_3^{(m)}$	$D_4^{(m)}$	$D_3^{(m+1)}$	$D_4^{(m+1)}$
Number of column to be replaced	I	I	3	3	2	2	4	4
Replacement column	I	II	I	II	I	II	I	II

$$\text{I} = \begin{bmatrix} c_3 \\ 0 \\ c_{10} \\ c_{15} \end{bmatrix} \qquad \text{II} = \begin{bmatrix} 0 \\ c_6 \\ c_{11} \\ c_{16} \end{bmatrix}.$$

The coefficients c_k are defined as follows:

$$
\begin{aligned}
&c_1 = k_{11}^{(m)} + s_{11}^{(m)} \quad c_2 = k_{12}^{(m)} \quad c_3 = k_3^{(m)} + s_{13}^{(m)} \quad c_4 = k_{11}^{(m+1)} + s_{11}^{(m+1)} \\
&c_5 = k_{12}^{(m+1)} \quad c_6 = k_{13}^{(m+1)} + s_{13}^{(m+1)} \quad c_7 = k_{21}^{(m)} \quad c_8 = k_{22}^{(m)} + s_{22}^{(m)} \\
&c_9 = s_{23}^{(m(m+1))} \quad c_{10} = k_{23}^{(m)} + s_{23}^{(mm)} \quad c_{11} = s_{23}^{(m(m+1))} \quad c_{12} = k_{21}^{(m+1)} \\
&c_{13} = s_{22}^{((m+1)m)} \quad c_{14} = k_{22}^{(m+1)} + s_{22}^{((m+1)(m+1))} \quad c_{15} = s_{23}^{((m+1)m)} \quad c_{16} = k_{23}^{(m+1)} + s_{23}^{((m+1)(m+1))}.
\end{aligned}
$$

APPENDIX C

The coefficients T_i in (16)

$$
\begin{aligned}
T_1 &= k_{33}^{(m)} + s_{33}^{(m)} + \bar{N}_1(m\pi\bar{h})^2 + s_{33}^{(mm)} - [k_{31}^{(m)} + s_{31}^{(m)}]R_1^{(m)} - [k_{32}^{(m)} + s_{32}^{(mm)}]R_3^{(m)} - s_{32}^{(m(m+1))}R_3^{(m+1)} \\
T_2 &= s_{33}^{(m(m+1))} - [k_{31}^{(m)} + s_{31}^{(m)}]R_2^{(m)} - [k_{32}^{(m)} + s_{32}^{(mm)}]R_4^{(m)} - s_{32}^{(m(m+1))}R_4^{(m-1)} - f_{33}\bar{M} \\
T_3 &= s_{33}^{((m+1)m)} - [k_{31}^{(m+1)} + s_{31}^{(m+1)}]R_1^{(m+1)} - [k_{32}^{(m+1)} + s_{32}^{((m+1)(m+1))}]R_3^{(m-1)} - s_{32}^{((m+1)m)}R_3^{(m)} + f_{33}\bar{M} \\
T_4 &= k_{33}^{(m+1)} + s_{33}^{(m+1)} + \bar{N}_1[(m+1)\pi\bar{h}]^2 + s_{33}^{((m+1)(m+1))} - [k_{33}^{(m+1)} + s_{31}^{(m+1)}]R_2^{(m+1)} \\
&\quad - [k_{32}^{(m+1)} + s_{32}^{((m+1)(m+1))}]R_4^{(m+1)} - s_{32}^{((m+1)m)}R_4^{(m)}.
\end{aligned}
$$

APPENDIX D

The coefficients $\bar{s}_{\alpha\beta}^{(i)}$ in (19)

$$
\begin{aligned}
\bar{s}_{11}^{(i)} &= (i\pi)^2\bar{h}\bar{E}_s\bar{A}_s/(\lambda^2\bar{I}_s) \\
\bar{s}_{13}^{(i)} &= (i\pi)^3\bar{z}_s\bar{h}^2\bar{E}_s\bar{A}_s/(\lambda^2\bar{I}_s) \\
\bar{s}_{22}^{(i)} &= n^2\bar{h}\bar{E}_r\bar{A}_r/\bar{I}_r \\
\bar{s}_{23}^{(i)} &= n\bar{h}(1 + n^2\bar{z}_r\lambda\bar{h})\bar{E}_r\bar{A}_r/\bar{I}_r \\
\bar{s}_{31}^{(i)} &= s_{13}^{(i)} \\
\bar{s}_{32}^{(i)} &= s_{23}^{(i)} \\
\bar{s}_{33}^{(i)} &= (\bar{h}/\bar{I}_r)[(i\pi n)^2\bar{G}_r\bar{J}_r + n^4\lambda^2\bar{E}_r\bar{I}_{0r} + \bar{E}_r\bar{A}_r(1 + 2n^2\bar{z}_r\lambda\bar{h})] + (\bar{h}/\bar{I}_s)[(i\pi n)^2\bar{G}_s\bar{J}_s + (i\pi)^4\bar{E}_s\bar{I}_{0s}/\lambda^2]
\end{aligned}
$$

$$\bar{I}_s = \bar{I}_s/L \qquad \bar{I}_r = \bar{I}_r/L.$$